A Thesis

entitled

Electrochemical Detection of SARS-CoV-2 Using Aryl Diazonium Salt Grafted Carbon Electrodes

by

Khalid Khalaf

Submitted to the Graduate Faculty as partial fulfillment of the requirements for the Master of Science Degree in Bioengineering

Dr. Yuan Tang, Committee Chair

Dr. Dong-Shik Kim, Committee Member

Dr. Brent Cameron, Committee Member

Dr. Scott C. Molitor, Acting Dean
College of Graduate Studies

The University of Toledo

August 2023

An Abstract of

Electrochemical Detection of SARS-CoV-2 Using Aryl Diazonium Salt Grafted Carbon Electrodes

by

Khalid Khalaf

Submitted to the Graduate Faculty as partial fulfillment of the requirements for the Master of Science Degree in Bioengineering

The University of Toledo
August 2023

This thesis presents a novel electrochemical biosensor for detecting SARS-CoV-2, the virus responsible for the global pandemic. Using aryl diazonium salt-grafted carbon electrodes, the biosensor offers a novel approach to virus detection. Using Electrochemical Impedance Spectroscopy (EIS) and Cyclic Voltammetry (CV), this study investigates the immobilization process of the aryl diazonium salt, ACE2 enzyme, and SARS-CoV-2 and verifies the efficacy of this process.

The biosensor exhibits a considerable response to variations in virus concentration, with the electron transfer process functioning most efficiently at the COVID stock concentration. In the cyclic voltammogram, the redox reactions of functional groups on SARS-CoV-2 provide a quantifiable redox response.

A comparative experiment establishes the biosensor's selectivity further, with SARS- CoV-2 exhibiting a larger oxidation and reduction peak in the CV measurements than H1N1. This study establishes the foundation for future research on the development of rapid, accurate, and cost-effective diagnostic tools for managing the current pandemic and potential future outbreak.

Contents

List of Figures

Chapter 1

1. Introduction

1.1 Background

The ongoing global pandemic caused by the Severe Acute Respiratory Syndrome Coronavirus 2 (SARS-CoV-2) has highlighted the importance of rapid, accurate, and readily accessible diagnostic techniques (Alafeef et al., 2020). Since its first appearance in late 2019, SARS-CoV-2 has caused millions of infections and fatalities and posed enormous challenges to public health systems around the globe. It has virtually spread to every corner of the globe. The SARS-CoV-2 virus is a coronavirus that belongs to the larger coronavirus family. Coronaviruses are a group of viruses that can produce a range of illnesses, from the common cold to more severe conditions. It is transmitted most frequently through the exchange of respiratory particles and through direct contact. Coronavirus disease 2019 (COVID-19) can be caused by infection with the virus, and its severity can range from mild symptoms to severe illness and mortality.

The reverse transcription polymerase chain reaction (RT-PCR) is currently the most prevalent method for diagnosing COVID-19 (Chaimayo et al., 2020). This method requires the collection of nasopharyngeal samples using probes, followed by the transfer of the virus to a solution and the extraction of RNA. The reverse transcription-polymerase chain reaction (RT-PCR) is a highly accurate technique; however, it is time-consuming, requires specialized apparatus and trained personnel, and can take several hours to several days to complete. Additionally, the high cost of PCR tests can be an impediment to extensive testing, especially in regions with limited resources.

In view of these obstacles, there is an urgent need for new diagnostic methods that are not only accurate but also rapid, inexpensive, and easy to implement. This has increased interest in the research and development of biosensors capable of detecting SARS-CoV-2 (Vadlamani et al., 2020). Biosensors, which are devices that integrate a biological recognition component with a signal transducer, may be able to meet these requirements. Several varieties of biosensors can provide rapid, on-site detection of viral antigens or antibodies and can be manufactured at a relatively low cost. As a result, they are a promising instrument for widespread testing, as they are relatively inexpensive to produce. In the course of our research, we utilized screen-printed carbon electrodes and an aryl diazonium salt solution to create a novel electrochemical biosensor for the detection of SARS-CoV-2. This strategy has the potential to provide rapid, accurate, and cost-effective detection of SARS-CoV-2, making it a viable alternative to the currently employed diagnostic procedures (Kronberg Jakobsen et al., 2021). This is our principal area of investigation.

Chapter 2

2. Problem Statement

The ongoing pandemic caused by SARS-CoV-2 has highlighted the critical need for rapid, accurate, and easily accessible diagnostic instruments. Currently, the reverse transcription polymerase chain reaction (RT-PCR) is the most prevalent method for COVID-19 diagnosis. Despite its high accuracy, RT-PCR has several limitations Including the need for specialized apparatus and trained personnel, the time-consuming nature of the process, and the high cost, which can be an impediment to widespread testing, particularly in settings with limited resources.

The current primary diagnostic method for SARS-CoV-2 is not readily scalable or available to all populations, especially in settings with limited resources. This issue has significant implications for pandemic management, as widespread testing is essential for tracking the spread of the virus, instituting appropriate public health measures, and ultimately controlling the pandemic.

Therefore, alternative diagnostic methods that are not only accurate but also rapid, cost-effective, and accessible are urgently required. These techniques should ideally not require specialized equipment or personnel with extensive training, and they should be suitable for point-of-care testing. This thesis seeks to address the problem of developing such a diagnostic instrument.

Chapter 3

3. Literature Review

3.1 Introduction to SARS-CoV-2 and ACE2

3.1.1 SARS-CoV-2 and ACE2 Interaction

The SARS-CoV-2 virus possesses a unique ability to bind to the angiotensin-converting enzyme 2 (ACE2) receptor on human cells, thereby gaining entry and initiating infection (Yan et al., 2020). This interaction is facilitated by the receptor-binding domain (RBD) of the spike (S) protein on the surface of the SARS-CoV-2 virus, which interacts directly with ACE2 (Tan et al., 2020).

Multiple human tissues express the ACE2 receptor, including the lungs, heart, kidneys, and intestines (Yan et al., 2020). The expression of ACE2 in these tissues may affect the severity and progression of COVID-19. High ACE2 expression in the lungs and heart, for instance, may explain the severe respiratory and cardiovascular complications observed in some COVID-19 patients (Yan et al., 2020).

Not only is the interaction between SARS-CoV-2 and ACE2 a key factor in the virus's capacity to infect a wide variety of tissues, but it is also a primary therapeutic target. Neutralizing antibodies capable of inhibiting the interaction between the spike protein and ACE2 have been developed, with promising laboratory results (Tan et al., 2020; Ejemel et al., 2020). These antibodies inhibit the virus' ability to enter cells by prohibiting it from binding to ACE2 (Tan et al., 2020; Ejemel et al., 2020).

Vaccine development also requires an understanding of the interaction between SARS-CoV-2 and ACE2. Several vaccine candidates intend to stimulate an immune response

against the spike protein, thereby inhibiting its ability to bind to ACE2 (Tan et al., 2020; Ejemel et al., 2020).

3.1.2 SARS-CoV-2 Structure and Function

The unique structure of the SARS-CoV-2 virus, which caused the COVID-19 pandemic, enables it to bond to and invade host cells. The virus is composed of multiple proteins, but the spike (S) protein is essential for the virus to infect host cells. The S protein is a trimeric glycoprotein that protrudes from the surface of the virus and lends it its distinctive "crown" appearance. The S protein is composed of two subunits: S1, which binds to the host cell receptor, and S2, which aids in the fusion of the viral and host cell membranes (Hoffmann et al., 2020).

A receptor-binding domain (RBD) on the S1 subunit recognizes and binds to the angiotensin-converting enzyme 2 (ACE2) receptor on the surface of host cells. This interaction is necessary for the virus to infect and enter host cells. This is one of the reasons why SARS-CoV-2 is more infectious than SARS-CoV (Shang et al., 2020).

Two heptad repeat regions (HR1 and HR2) within the S2 subunit of the S protein are essential for the fusion of the viral and host cell membranes. After the S1 subunit binds to the ACE2 receptor, the S2 subunit undergoes a conformational change that facilitates the fusion and entry of the virus into the host cell by bringing the viral and host cell membranes closer together (Xia et al., 2020).

Not only is the interaction between the S protein and the ACE2 receptor essential for the virus to infect host cells, but it also has implications for the development of therapeutic interventions. For instance, pharmaceuticals that inhibit the interaction between the S protein and the ACE2 receptor may prevent the virus from infecting and entering host cells. Vaccines that stimulate the immune system to produce antibodies against the S protein may also prevent the virus from infecting host cells (Tai et al., 2020).

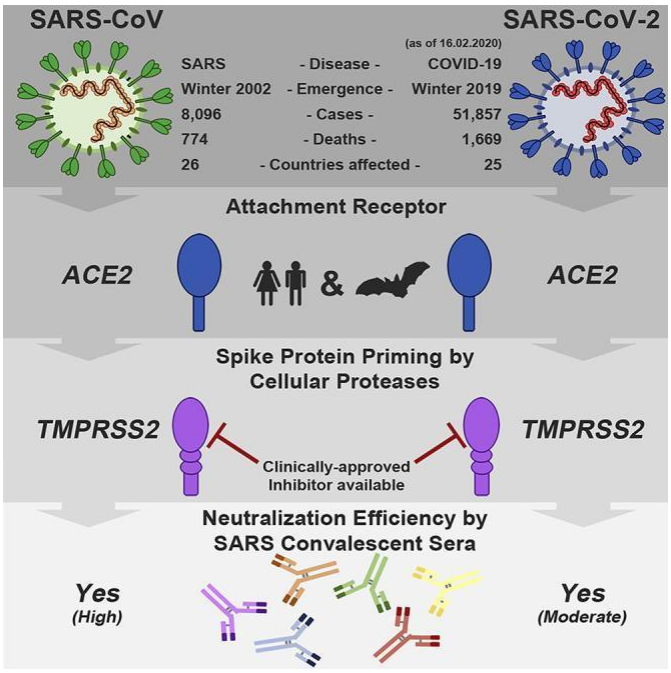

Figure 1 Depiction of ACE2 and TMPRSS2 Spike Protein Interaction (Hoffmann et al., 2020b)

3.1.3 ACE2 and COVID-19 Severity

Multiple factors, including older age, comorbidities, and male sex, have been associated with the severity of COVID-19. However, the function of ACE2 in the severity of disease is still being investigated. Asselta and colleagues investigated the expression levels and genetic variants of the ACE2 and TMPRSS2 genes in an Italian cohort because these genes are essential for SARS-CoV-2 infection (2020). The study found no significant association between ACE2 and disease severity or gender bias. However, it was discovered that TMPRSS2 levels and genetic variants could potentially modulate disease severity, indicating the need for additional research in this area.

ACE2 is one of the genes that evade X-chromosome inactivation and exhibits a heterogeneous pattern of male-female expression, with higher expression in males in several tissues . Regarding the lung, the principal target of SARS-CoV-2, the study found no significant differences in ACE2 transcript levels between males and females, nor between younger and older females. This suggests that the role of ACE2 in COVID-19 severity is not necessarily proportional to its lung expression levels.

Genetic variation is another aspect of ACE2 that could potentially influence COVID-19 severity. Comparing the Italian population with those of Europe and East Asia, Asselta and colleagues discovered no statistically significant differences in the prevalence of rare deleterious variants in ACE2 (2020). Nonetheless, their results yielded a significant difference in the frequency of the single nucleotide polymorphism (SNP) rs2285666, with the frequency of the rare A allele being 0.2% in Italians and Europeans and 0.5% in East Asians this variant has been investigated as a potential risk factor for hypertension, type 2 diabetes, and coronary artery disease, which are observed frequently in COVID-19 patients. Therefore, it is conceivable that genetic variation in ACE2 could indirectly affect the severity of COVID-19 by influencing these comorbidities.

While ACE2 plays a crucial role in SARS-CoV-2 infection, its function in COVID-19 severity is likely to involve multiple factors, including genetic variation and interaction with other genes such as TMPRSS2. To thoroughly comprehend these relationships and their implications for patient care and treatment, additional research is required.

3.2 Current Detection Methods for SARS-CoV-2

3.2.1 Introduction to SARS-CoV-2 Detection Methods

The gold standard for detecting SARS-CoV-2 infection cases is the Reverse Transcription Quantitative Polymerase Chain Reaction (RT-qPCR). Since its discovery in the 1990s, this technique for diagnosing infectious diseases has become well-established and the most widely used (Zhang et al., 2020). Since its discovery decades ago, RT-qPCR has undergone a profound evolution. For detection and relative quantification, quantitative real-time PCR (qPCR) has replaced the analogous qualitative conventional PCR that uses gel electrophoresis. The third generation of PCR, digital PCR (dPCR), was devised to precisely quantify pathogens without the need for a standard curve (Zhang et al., 2020).

Droplet Digital PCR (ddPCR) is a third-generation PCR technique that provides absolute DNA or RNA molecule quantification. It has the capacity to divide samples into thousands of droplets for direct detection and quantification. Recent publications have demonstrated the superiority of dPCR over RT-PCR for the detection and quantification of targets, including SARS-CoV-2. Suo et al. demonstrated in their publication that dPCR could detect SARS-CoV-2 in clinical samples that had previously tested negative by RT-PCR. This meant that the assay's detection capabilities were superior to those of RT-PCR and that it was able to avoid the false-negative results that RT-PCR generated (Zhang et al., 2020).

Similar to RT-PCR, digital PCR allows for multiplexing. Using probe-based or Evagreen assays, multiple assays can be designed to quantify multiple targets in a single well. This has been emphasized in order to reduce the cost of simplex assays and increase the likelihood of target detection (Zhang et al., 2020). Despite RT-qPCR being the gold standard for diagnosing COVID-19 infection, according to research by Falzone et al. (2020)., due to pre-analytical and technical limitations, low viral load samples are frequently misdiagnosed as false-negative samples.

Falzone et al. (2020) compared the sensitivity of RT-qPCR and droplet digital PCR (ddPCR) for detecting SARS-CoV-2 in samples from two individuals diagnosed with COVID-19 positivity and negativity. RT-qPCR was unable to identify positive samples with a low viral burden, whereas ddPCR demonstrated a higher sensitivity rate than RT-qPCR. Even at a 10-fold dilution, both EvaGreen and probe ddPCR were able to identify the sample with a low viral load as positive.

Moreover, Falzone et al. (2020) suggested that ddPCR is firmly recommended in clinical practice for the diagnosis of COVID-19 and the follow-up of positive patients until complete remission due to its increased sensitivity and specificity in comparison to RT-qPCR.

Suo et al. (2020) found that RT-qPCR had a false-negative rate of 28.6% when detecting SARS-CoV-2 from pharyngeal swab samples, whereas ddPCR had a significantly reduced false-negative rate of 7.4%. These results suggest that ddPCR may be a more reliable method for detecting SARS-CoV-2, particularly in samples with a low viral burden, which could lead to more accurate diagnosis and improved patient care.

3.2.2 RT-qPCR for SARS-CoV-2 Detection

Due to its high sensitivity and specificity, RT-qPCR (Real-Time Quantitative Polymerase Chain Reaction) has been widely utilized for the detection of SARS-CoV-2. This technique amplifies viral RNA sequences, which are subsequently detected and quantified in real-time. The RT-qPCR technique focuses on particular regions of the SARS-CoV-2 genome, most frequently the N (nucleocapsid), E (envelope), and RdRP (RNA-dependent RNA polymerase) genes (Barra GB et al., 2020).

Barra GB et al. (2020) evaluated the analytical efficacy of the Charité and CDC protocols for SARS-CoV-2 detection using RT-qPCR. The N1 assay, which targets the N gene, exhibited the maximum analytical sensitivity for its RNA targets, with a detection limit of 21 copies/reaction, according to the study. The RdRP (modified) assay, which targets the RdRP gene, also demonstrated excellent analytical sensitivity, with a detection limit of 33.7 copies/reaction. The E assay, which targets the E gene, was determined to be a tertiary assay with a detection limit of 141 copies/reaction.

Additionally, the study revealed that the N1 assay yielded more positive results than the E assay, and that the E assay yielded more positive results than the RdRP (modified) assay. This may be due to differences in the abundance of the target in the sample due to the presence of cellular material. Upon cell entry, SARS-CoV-2 hijacks 60% of the cell's expression capacity, and its replication is dependent not only on the production of genomic RNA but also on the expression of several shorter subgenomic RNAs encoding for conserved structural proteins essential for the assembly of progeny virions. RdRP is located on ORF1b, and its expression requires ribosomal frameshifting, indicating that it

is produced at substantially lower levels than ORF1a-encoded functions and subgenomic RNA. Therefore, the RdRP copy number in the sample's cellular content is lesser than E and N1. In contrast, the E and N1 targets are highly expressed, particularly the N gene, as its sequences are present in nearly all subgenomic RNA (Barra GB et al., 2020).The RT-qPCR method, particularly the N1 assay, has proven to be a reliable and sensitive technique for detecting SARS-CoV-2.

3.2.4 Comparison of RT-qPCR and ddPCR

Multiple studies have determined that RT-qPCR and ddPCR are both effective methods for detecting SARS-CoV-2, but they each have their own advantages and disadvantages. RT-qPCR is the most common method for detecting SARS-CoV-2 due to its high sensitivity, specificity, and speed (Corman et al., 2020). RT-qPCR may have limitations in detecting low viral loads, which can contribute to false-negative results (Tom et al., 2020).

ddPCR has a greater sensitivity than RT-qPCR, making it more effective at detecting low viral concentrations (Yu et al., 2020). This makes ddPCR a potentially more reliable method for detecting SARS-CoV-2, particularly in cases with a low viral burden. However, ddPCR is more time-consuming and requires more specialized apparatus than RT-qPCR, limiting its applicability in certain settings (Suo et al., 2020).

Falzone et al. (2020) compared the efficacy of RT-qPCR and ddPCR in detecting SARS-CoV-2 and discovered that ddPCR was more sensitive and accurate than RT-qPCR, particularly when analyzing samples with low viral loads. However, the study also revealed that RT-qPCR was more efficient and better suited for high-throughput testing.

In a separate study, researchers discovered that RT-qPCR and ddPCR had comparable detection rates for SARS-CoV-2, but ddPCR was more accurate at quantifying viral load (Lu et al., 2020). This suggests that while both techniques are effective for detecting

SARS-CoV-2, ddPCR may provide more precise information regarding the amount of virus present in a sample.

Even though RT-qPCR and ddPCR are both effective methodologies for detecting SARS-CoV-2, each has distinct advantages and disadvantages. The choice between these two techniques may hinge on the testing situation, such as the need for rapidity, sensitivity, or precision in quantifying viral load.

3.3 Electrochemical Detection of Viruses

3.3.1 Electrochemical Detection

Due to the absence of swift, accurate, and user-friendly detection methods, detecting viral infections has been a significant challenge (Divya et al., 2022). Traditional diagnostic techniques frequently necessitate extensive infrastructure and financial resources, which are not always readily available in all contexts. Recent research has focused on the development of biosensors, primarily electrochemical biosensors, for virus detection in order to overcome these obstacles.

Electrochemical biosensors have demonstrated promising sensitivity, selectivity, and speed of diagnosis (Imran et al., 2021). These devices function by recognizing specific biological elements, such as aptamers, and converting this recognition into a measurable and analyzable electrical signal. Particularly, aptamers have emerged as efficient biorecognition elements for the detection of a variety of analytes, including viruses (Divya et al., 2022). These biosensors can be designed as labeled or label-free, each with their own benefits and drawbacks.

In addition to their inherent capabilities, advances in data processing techniques, such as machine learning and deep learning, have further improved the diagnostic accuracy of electrochemical biosensors. Gecgel et al. (2022) successfully diagnosed SARS-CoV-2

samples with high sensitivity, specificity, and accuracy by applying deep learning techniques to data acquired from an ultra-fast COVID-19 diagnostic sensor.

In addition, the portability of these biosensors has contributed significantly to their potential for extensive application. Portable electrochemical biosensors based on microcontrollers allow for on-site testing without the need for centralized laboratories, allowing for high-throughput and accurate measurements (Abdul Ghani et al., 2022). The addition of portable potentiostats and microfluidics chambers to these devices creates a miniature lab that can be utilized in a variety of contexts.

The development and application of electrochemical biosensors for virus detection represent a promising strategy for addressing the limitations of conventional diagnostic techniques. Through the incorporation of biorecognition elements, advanced data processing techniques, and portable designs, these devices have the potential to detect viral infections quickly, accurately, and easily.

3.3.2 Use of PDFT as a SAM for Detection

According to a study by Vezza. V et al, perfluorodecanethiol (PFDT) has been recognized as a highly promising material for the advancement of self-assembled monolayers (SAMs) in the field of electrochemical biosensors. The study utilized PFDT to create a self-assembled monolayer (SAM) on a gold sensor surface, serving as a foundation for the attachment of the ACE2 enzyme. This enzyme acts as the recognition element for the detection of SARS-CoV-2. The impact of the PFDT SAM layer on the charge transfer resistance (RCT), a widely utilized signal parameter in impedimetric biosensor measurements, was investigated. The enhanced rate of charge transfer (RCT) observed in this study was significantly augmented upon the physisorption of the ACE2 enzyme into the PFDT material, providing evidence of successful immobilization of the enzyme onto the surface of the sensor.

The utilization of PFDT as a self-assembled monolayer (SAM) presents numerous benefits in the advancement of biosensors. The PFDT SAM layer was determined to be highly suitable for enzyme retention through amphiphobic interactions. The PFDT SAM layer has the potential to enhance the stability and reliability of biosensors through its anti-biofouling properties. The study focuses on the preparation procedure for functionalizing the PFDT-ACE sensor and its application in virus binding. The procedure involves two stages: deposition of PFDT on a cost-effective PCB electrode and functionalization of ACE2 through physisorption into the PFDT. The enhanced practicality of the assay is attributed to its simplicity, which expedites the time to obtain results. Additionally, this simplicity has the potential to facilitate storage, transportation, and prolong the shelf life of the assay. This is due to the fact that sensor strips can be shipped without the need for preprinting the ACE2 enzyme. The utilization of PFDT as a surface modification technique in the fabrication of the biosensor not only enhances the sensor's sensitivity and specificity but also holds significant implications for its scalability and cost-effectiveness. The approach outlined in the study has the potential to be efficiently implemented in a glucose test strip production setting, thereby potentially achieving a highly economical solution. (Vezza.V et al 2021)

Chapter 4

4. Materials and Methods

4.1 Required Materials

The materials used in the experiments came from a variety of sources. The screen-printed gold and carbon electrodes were acquired from Pine Research. For the modification of the gold electrode, Sigma Aldrich provided the Perfluorodecanethiol (PFDT). For the modification of the carbon electrode, a solution of Aryl Diazonium salt. 1-Ethyl-3-(3-dimethylaminopropyl)carbodiimide (EDC) and N-Hydroxysuccinimide (NHS) for the activation of carboxyl groups. The Angiotensin-Converting Enzyme 2 (ACE2) enzyme was obtained from Sigma Aldrich for the immobilization phase.

The SARS-CoV-2 used for incubation was obtained from Fisher Scientific. The virus was managed in accordance with the applicable biosafety level guidelines. Similarly, Fisher Scientific also supplied the H1N1 virus used in the comparative gold electrode investigations. 0.1N sulfuric acid used for cleansing the carbon electrode. Utilizing a standard water deionization system, deionized water for cleaning the electrodes. For the electrochemical measurements, a 5 mM $[Fe(CN)_6]^{3-/4-}$ solution was prepared using 0.1 M phosphate buffer solution (PBS, pH 7.2) and 0.1 M KCl. All materials were utilized without any additional purification.

4.2 Preparation of Electrodes

The investigations were carried out using gold and carbon screen-printed electrodes. Prior to any modification, both types of electrodes were subjected to a comprehensive cleaning procedure to ensure that any contaminants that could potentially interfere with the subsequent steps were eliminated. The cleaning procedure for the gold screen-printed electrode consisted of a simple rinse with deionized water followed by drying with

compressed air. Before the formation of the self-assembled monolayer (SAM) of PFDT, it was essential that the surface of the electrode was devoid of impurities.

Different material properties necessitated a more rigorous cleansing procedure for the carbon screen-printed electrode. The electrode was initially submerged in 0.1N sulfuric acid and a CV cleaning Cycle. This phase served to clean the surface of the electrode and produce a more uniform and reactive surface for the subsequent grafting of the Aryl Diazonium salt. After being treated with acid, the electrode was thoroughly rinsed with deionized water and then dried with compressed air. In both instances, the cleanliness of the electrode surfaces was of the uttermost importance, as any residual contaminants could interfere with the electrode modifications and result in inconsistent or inaccurate electrochemical measurements.

4.3 Modification of Electrodes

Two distinct procedures were used to modify the electrodes, corresponding to the two categories of electrodes used: gold and carbon.

4.3.1 Gold Electrode Modification With PFDT

The gold screen-printed electrode was immersed for 24 hours in a solution of PFDT. This step enabled the formation of a self-assembled monolayer (SAM) of PFDT on the gold electrode surface. The SAM facilitates the ensuing immobilization of the ACE2 enzyme. After 24 hours, the electrode was extracted from the PFDT solution, thoroughly washed with deionized water to remove any unbound PFDT, and dried with compressed air.

4.3.2 Carbon Electrode Modification with Aryl Diazonium

The cleaned screen-printed carbon electrode was submerged in the Aryl Diazonium solution. The CV cycle for grafting the Aryl Diazonium was run. This provided the functional groups necessary for subsequent activation with EDC/NHS and immobilization of the ACE2 enzyme. The electrode was then removed from the Aryl

Diazonium salt solution, thoroughly rinsed with deionized water to remove any ungrafted Aryl Diazonium, and dried with compressed air.

Cyclic voltammetry (CV) and electrochemical impedance spectroscopy (EIS) in a 5 mM $[Fe(CN)_6]^{3-/4-}$ solution confirmed the successful modification of the electrodes in both instances. These electrochemical measurements demonstrated the formation of PFDT SAM on the gold electrode and the grafting of Aryl Diazonium onto the carbon electrode.

4.4 Immobilization of ACE2

Following the modification of the electrodes, immobilization of the ACE2 enzyme onto the modified surfaces was the next step. This procedure was executed differentially for the two types of electrodes.

4.4.1 Gold Electrode (PFDT)

The ACE2 enzyme was immobilized directly onto the surface of the gold electrode modified with PFDT. The gold electrode was left overnight in a small beaker of PFDT filled to the level of the working electrode. This allowed the ACE2 enzyme to bind to the PFDT SAM, thereby generating a stable and functional surface for subsequent incubation of the SARS-CoV-2 virus.

4.4.2 Carbon Electrode (Aryl Diazonium)

Prior to immobilizing the ACE2 enzyme, an additional step was required for the carbon electrode modified with Aryl Diazonium. The Aryl Diazonium-grafted carbon electrode was drop-cast with 15 µL of EDC/NHS solution and left for one hour. This step served to activate the surface carboxyl groups, which are required for subsequent immobilization of the ACE2 enzyme. After activation, the electrode was cleaned with deionized water and desiccated with compressed air. 15 µL of the ACE2 enzyme solution was then drop-cast onto the activated surface and left overnight to immobilize.

Cyclic voltammetry (CV) and electrochemical impedance spectroscopy (EIS) in an electrolyte solution confirmed the successful immobilization of the ACE2 enzyme in both instances. These electrochemical measurements provided evidence that the ACE2 enzyme was successfully immobilized on both types of electrodes.

4.5 Virus Incubation

Next, the SARS-CoV-2 virus was incubated on the modified and functionalized electrodes, following the immobilization of the ACE2 enzyme. For both electrodes, this procedure was executed identically, however the incubation time differed.

A volume of 15 µL of the SARS-CoV-2 virus solution was drop-cast onto the surface of the PFDT-modified gold electrode and the Aryl Diazonium-grafted carbon electrode. The virus was then allowed to incubate on the surface for a predetermined amount of time. Incubation for the gold electrode lasted 1 hour (Vezza. V et al 2021). Based on the optimal detection time determined through preliminary experiments for the carbon electrode, the incubation period was 12 hours.

During the incubation period, the SARS-CoV-2 virus binds to the immobilized ACE2 enzyme, simulating the interaction that occurs during the human infection process caused by the SARS-CoV-2 affinity to the spike protein. After the incubation period, the electrodes were washed with deionized water and dried with compressed air to eliminate any virus particles that had not been bound. CV and EIS were run in order to confirm whether detection has taken place.

4.6 Electrochemical Measurements

The electrochemical measurements were conducted using Cyclic Voltammetry (CV) under different conditions for various components of the biosensor:

5 mM $[Fe(CN)_6]^{3-/4-}$ Electrolyte Solution: The CV measurement for the electrolyte solution was conducted in the potential range from -0.8V to 0.8V. The base scan rate was

set at 100 mV/s, with a step size of 5 mV. The process was repeated for 5 cycles to ensure consistent results.

Carbon Electrode Cleaning: The cleaning of the carbon electrode was performed using 0.1N Sulfuric Acid. The CV measurement for this process was conducted in the potential range from -1.2V to 1.2V. The scan rate was set at 200 mV/s, with a step size of 5 mV. This process was also repeated for 5 cycles to ensure thorough cleaning of the electrode.

Aryl Grafting on Carbon Electrode: The grafting of aryl diazonium on the carbon electrode was achieved by submerging the electrode in a solution of aryl diazonium. The CV measurement for this process was conducted in the potential range from -1V to 0V. The scan rate was set at 200 mV/s, with a step size of 5 mV. This process was repeated for 15 cycles to ensure effective grafting of the aryl diazonium on the electrode.

4.7 Experimental Schematic

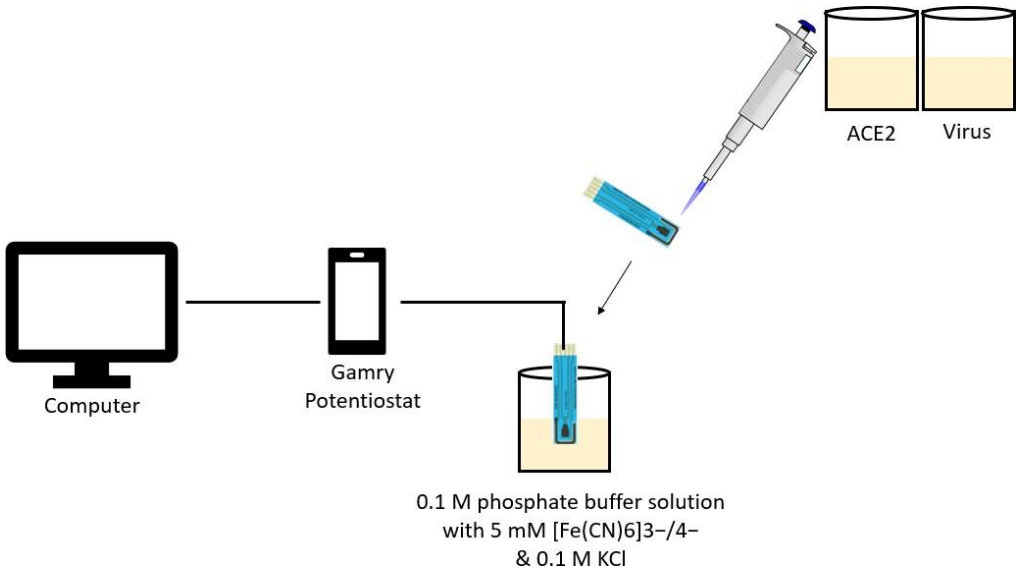

Figure 2 Schmatic of Virus detection using Gamry Potentiostat and Electrode

The experimental setup utilized for the electrochemical measurements encompasses a precisely defined system consisting of an electrode, electrolyte solution, a potentiostat, and a computer equipped with the requisite software. The immersion of the electrode in the electrolyte solution is a crucial aspect of the biosensor, as the electrode serves as the central component of the device. The solution utilized in this study functions as the medium for facilitating electrochemical reactions, while also serving as the carrier for the analyte under investigation, specifically SARS-CoV-2. The electrode is modified with a SAM of PFDT and the ACE2 enzyme, serving as the recognition element for SARS-CoV-2. The potentiostat, specifically a Gamry machine, is utilized to establish a connection with the electrode. The potentiostat plays a pivotal role in the experimental setup by regulating the voltage between the electrode and the reference electrode, as well as quantifying the current passing through the electrode. The generation of electrochemical signals enables the analysis and detection of the presence and concentration of SARS-CoV-2.

The potentiostat is connected to a computer running the Gamry software for data acquisition and analysis. The purpose of this software is to effectively manage the potentiostat and facilitate the acquisition and analysis of electrochemical data. This study utilizes the software's capability to perform both Cyclic Voltammetry (CV) and Electrochemical Impedance Spectroscopy (EIS), which are the primary techniques employed for the detection of SARS-CoV-2. The present study presents a well-designed experimental schematic that offers a concise and effective setup for the electrochemical detection of SARS-CoV-2. The utilization of a clearly defined system enables the attainment of precise control over experimental conditions and enhances the acquisition of accurate and dependable data.

Chapter 5

5. Results and Discussion

5.1 The electrochemical response of the modified sensor using PFDT to SARS-CoV-2

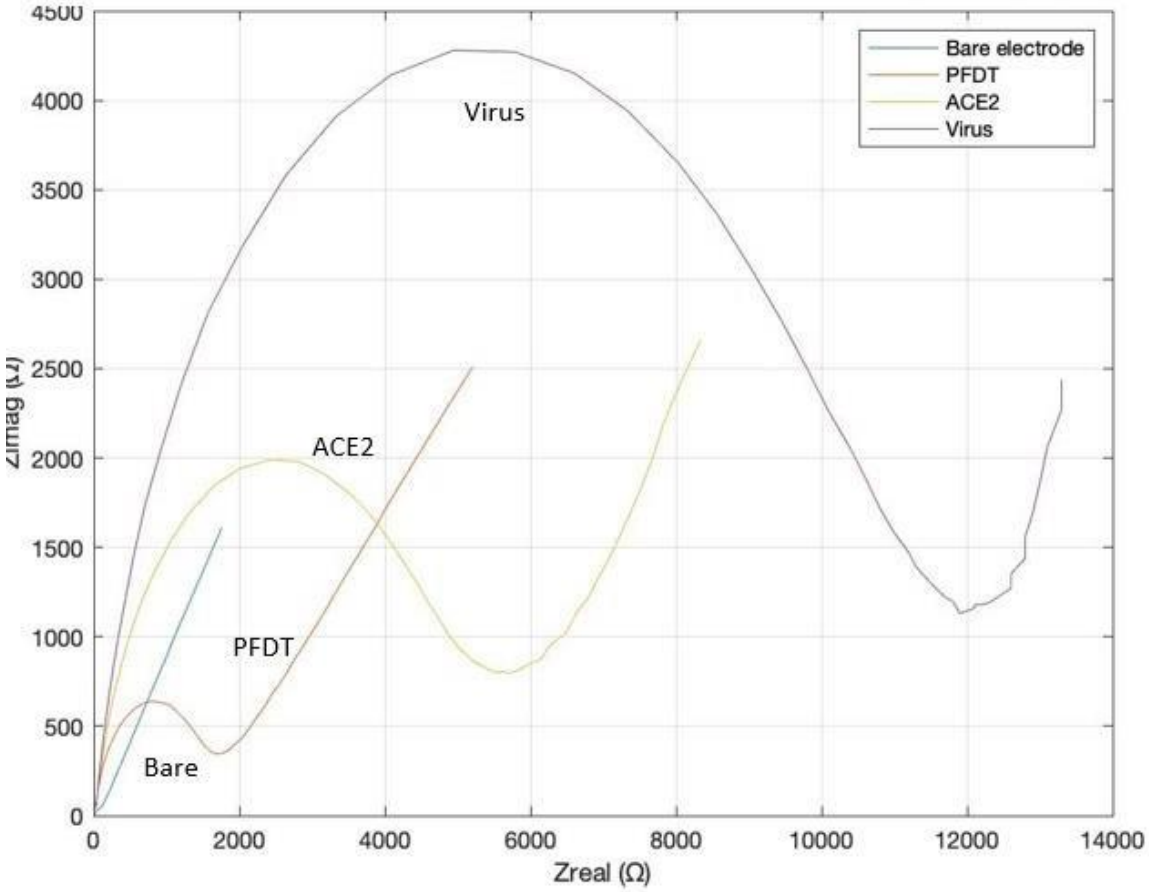

Figure 3 EIS graph of the Electrochemical Response of the Sensor Using PFDT to detect SARS-CoV-2

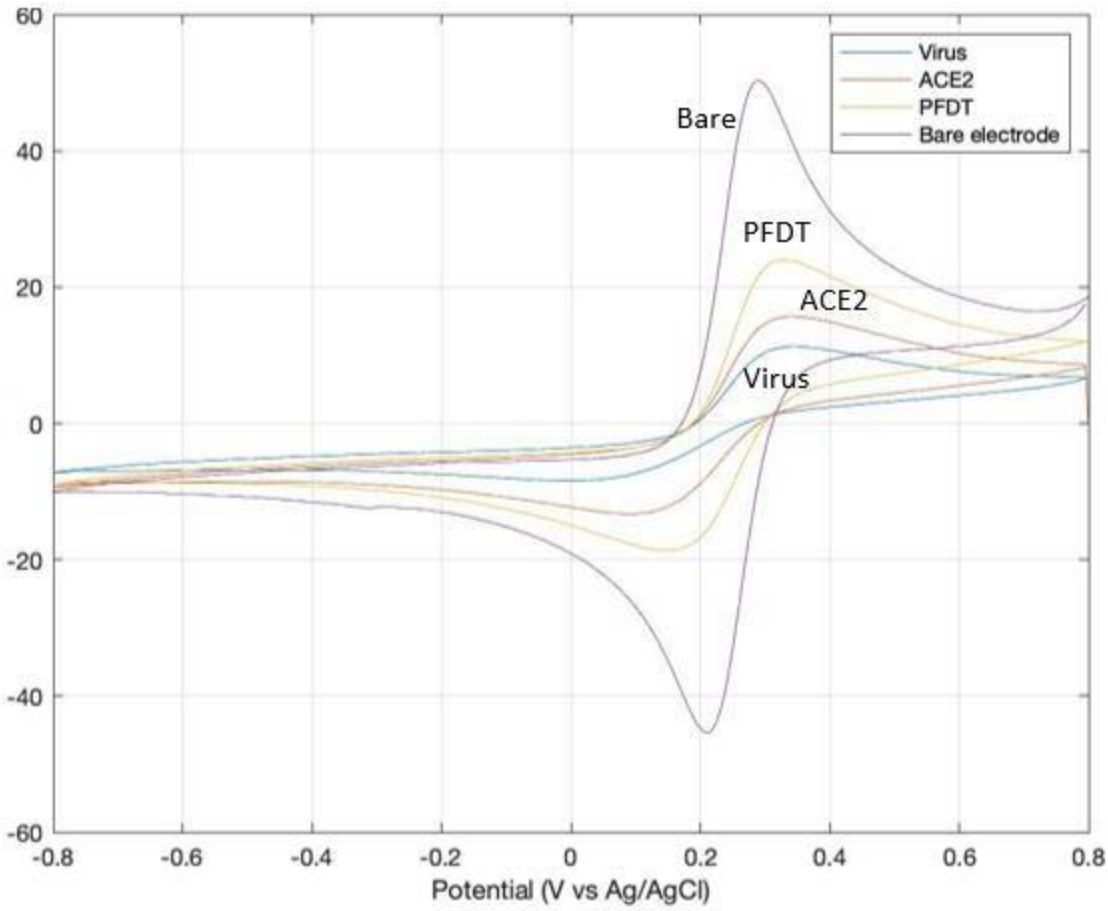

Figure 4 CV graph of the Electrochemical Response of the Sensor Using PFDT to detect SARS-CoV-2

Electrochemical impedance spectroscopy (EIS) and Cyclic voltammetry (CV) were performed in a 0.1 M phosphate buffer solution (PBS, pH 7.2), with 5 mM $[Fe(CN)_6]^{3-/4-}$ acting as the redox probe and 0.1 M KCl to investigate the interaction between the SARS-CoV-2 and the ACE2 enzyme immobilized on a gold electrode surface modified with PFDT.

The EIS tests were conducted within a frequency spectrum ranging from 0.1 Hz to 100,000 Hz, applying an alternating current voltage of 5 mV and a direct current voltage of 0.23 V. In Nyquist plots, the section that appears linear at lower frequencies is indicative of a diffusion-limited process, whereas a semicircular portion seen at higher frequencies signifies a charge transfer-limited process. Additionally, the diameter of the semicircle at these higher frequencies provides insight into the resistance of interfacial

charge transfer (R_{ct}). As more layers were added to the electrode surface, the Nyquist plots derived from the EIS measurements revealed intriguing trends with regard to the R_{ct}. The absence of a semicircle in the Nyquist plot for the bare gold electrode suggests that the electron transfer process was highly efficient, most likely due to the lack of insulating layers on the electrode surface (Mahmoud et al., 2008). R_{ct} increased when the PFDT layer was added, indicating that the PFDT layer impeded electron transfer to some degree. The formation of an insulating layer on the electrode surface by PFDT, a type of self-assembled monolayer (SAM), can increase the charge transfer resistance (Heo et al., 2012). The addition of the ACE2 enzyme increased R_{ct}, indicating that the enzyme layer added another layer of insulation to the electrode surface, further impeding the electron transfer process. This is consistent with previous research (Jarocka et al., 2014) that reported an increase in R_{ct} upon the attachment of a protein layer to a biosensor surface. The addition of the virus caused the greatest increase in R_{ct}, indicating that the virus layer added the greatest amount of insulation to the electrode surface, thereby impeding the electron transfer process the most. This is consistent with previous studies (Kaushik et al., 2018) that reported an increase in R_{ct} upon detection of a virus using an electrochemical biosensor.

The CV analyses were conducted in the potential range of −0.8 V to 0.8 V with a scan rate of 100 mV/s. The EIS findings align with those from the CV, where the unmodified electrode exhibits the highest current signal. Conversely, when the virus is immobilized on the ACE2 enzyme, the current signal is at its lowest. These results shed light on the electrochemical behavior of layered biosensors and demonstrate the affinity of ACE2 enzyme to SARS-CoV-2.

5.2 The electrochemical response of the proposed sensor using aryl diazonium salt to SARS-CoV-2

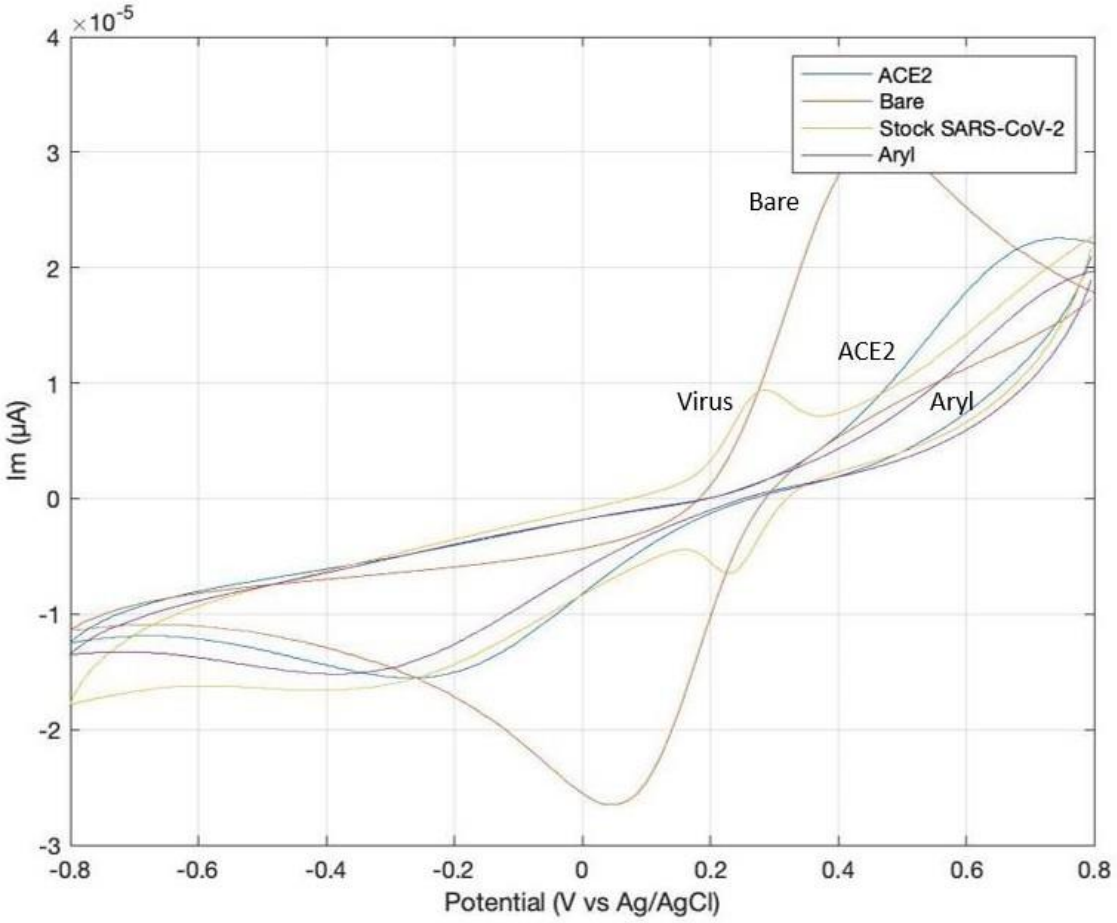

Figure 5 CV Graph depicting the electrochemical response of SARS-CoV-2 detection using Aryl Diazonium

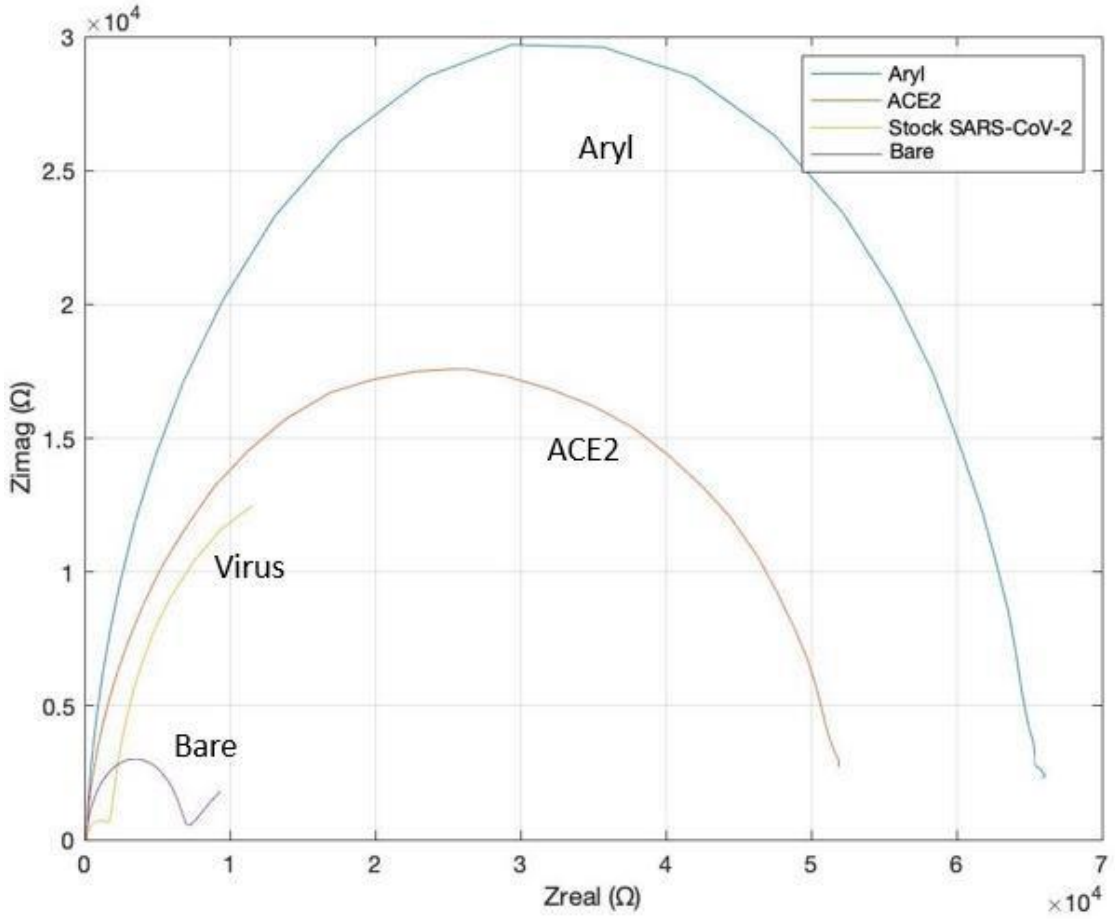

Figure 6 EIS Graph depicting the electrochemical response of SARS-CoV-2 detection using Aryl Diazonium

Each stage of electrode functionalization was examined using CV and EIS techniques. As seen in the cyclic voltammograms of Figure 5, the orange curve represents the current response of the unmodified electrode, which noticeably drops upon introducing the aryl diazonium salt (purple curve), confirming its successful formation. Following the electrodeposition of the aryl diazonium salt, there is a substantial current reduction, attributed to the non-conductive layer of the salt on the electrode surface. This salt layer impedes the electron transfer rate between the electrolyte solution and electrode surface, resulting in a significant current drop (Ghaedamini et. Al 2023). The ACE2 enzyme is characterized by the presence of oxygenated functional groups. These groups have the capacity to engage in redox reactions or charge transfer processes on the surface of the electrode, thereby enhancing electron transfer. More likely, it is the oxygenated

functional groups of the SARS-CoV-2 virus, once immobilized on the ACE2 enzyme, that take part in the redox reaction. This participation culminates in the emergence of a distinct redox peak.

EIS was additionally utilized to validate the effective immobilization of the aryl diazonium salt, ACE2 enzyme, and SARS-CoV-2, respectively. Figure 6 illustrates the EIS results for the bare electrode, the electrode modified with aryl diazonium salt, the electrode further modified with the ACE2 enzyme, and finally, the electrode with SARS-CoV-2 attached. The CV results are consistent with the EIS results. Following the modification with aryl diazonium salt, there was a significant increase in the R_{ct}, as shown by the red curve. The enlarged diameter observed for the aryl diazonium-modified electrode, the most extensive among all, can be attributed to the organic salt layer on the electrode, which acts as a barrier to electron transfer, hence increasing the electrode impedance. Conversely, the semicircle diameter begins to decrease with the subsequent steps. First, the immobilization of the ACE2 enzyme onto the aryl diazonium layer results in a decreased diameter. This decrease continues when the SARS-CoV-2 is then bound to the ACE2 enzyme, further reducing the semicircle diameter.

In the case of PFDT, the manner in which the ACE2 enzyme binds to the PFDT layer could be impacting the electron transfer process. If the enzyme molecule molecules are oriented in a way that covers up a large part of their oxygenated functional groups, then the potential facilitation of electron transfer by these groups could be hindered.

5.3 Optimal SARS-CoV-2 Incubation Time

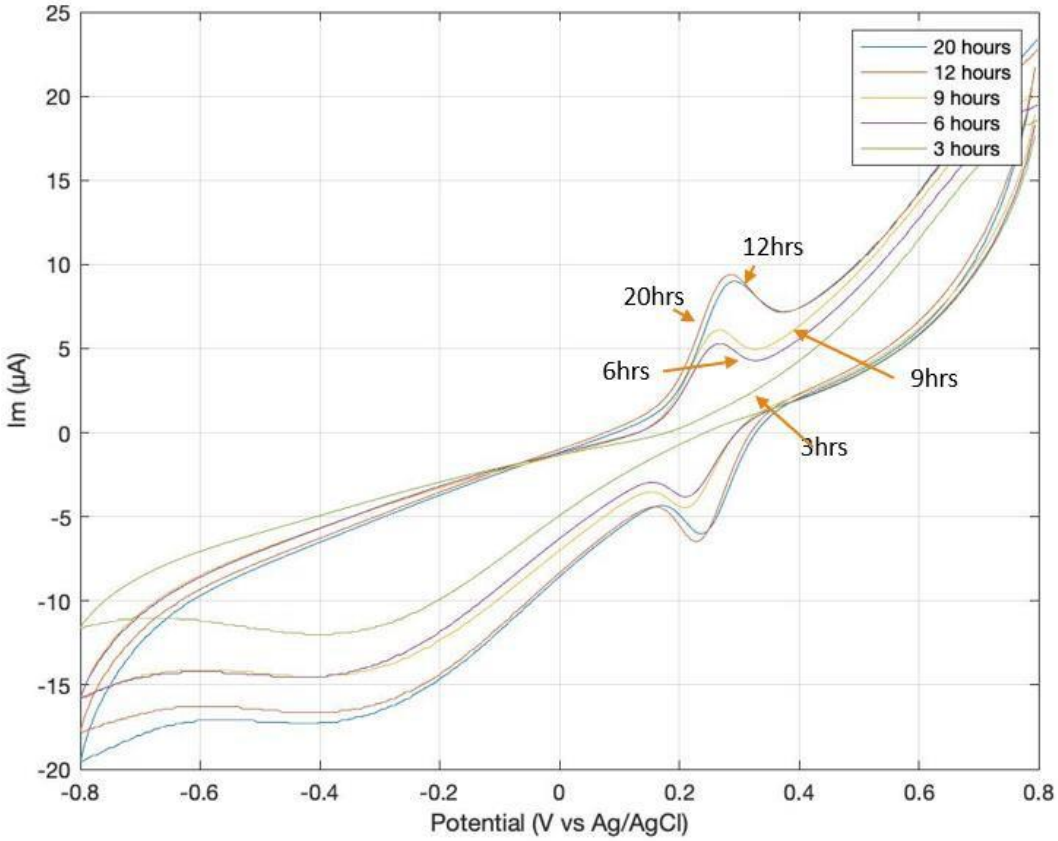

Figure 7 CV Graph of SARS-CoV-2 Incubation at 20, 12, 9, 6 and 3 Hours

The stock solution of SARS-CoV-2 was subjected to CV analysis to establish the most suitable incubation time for the virus. As illustrated in Figure 7, a three-hour incubation time does not present any redox peaks in the cyclic voltammogram. As the incubation time extends to 12 hours, the redox response augments, likely due to increased interaction time between the immobilized ACE2 enzyme and SARS-CoV-2 molecules. Conversely, extending the incubation time to 20 hours does not significantly alter the redox peaks, possibly due to saturation of the ACE2 enzyme with SARS-CoV-2 molecules. As such, the optimum incubation time for SARS-CoV-2 was determined to be 12 hours.

5.4 The sensor response to different concentration of SARS-CoV-2

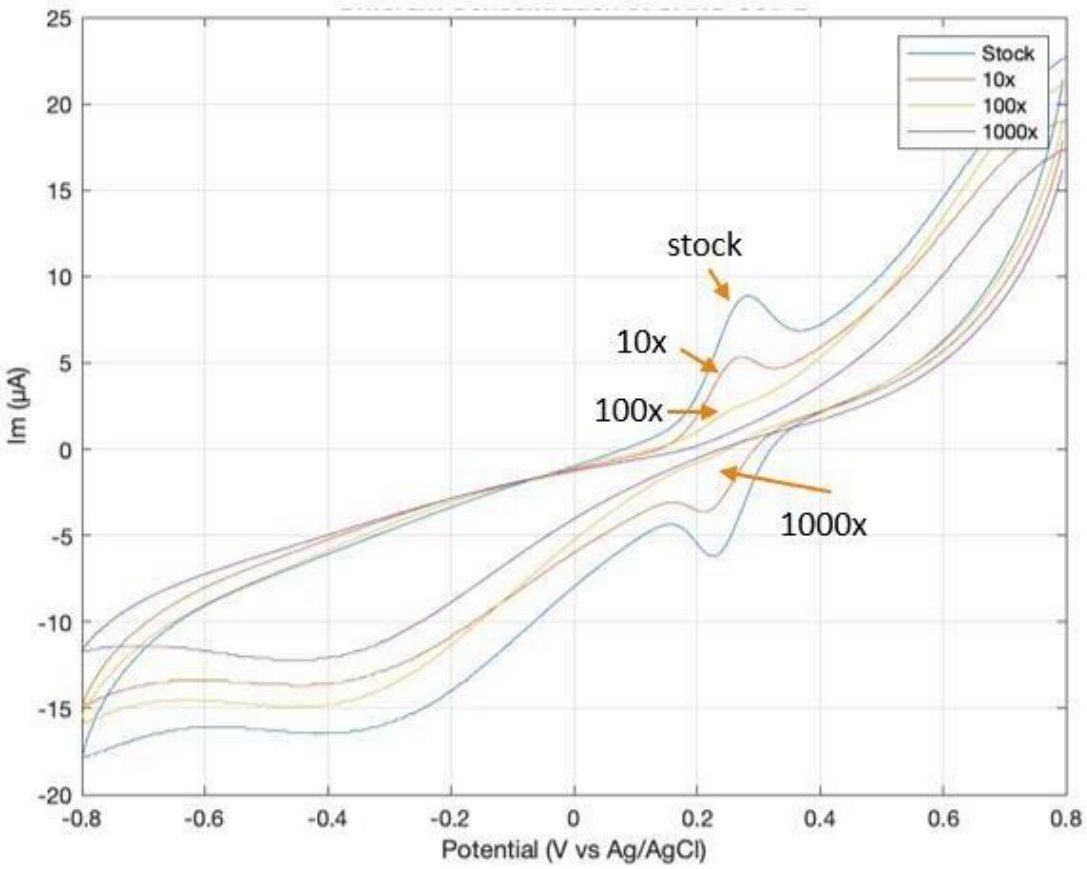

Figure 8 CV Graph of the Electrochemical Response of SARS-CoV-2 Detection at Stock, 10x, 100x and 1000x Dilutions

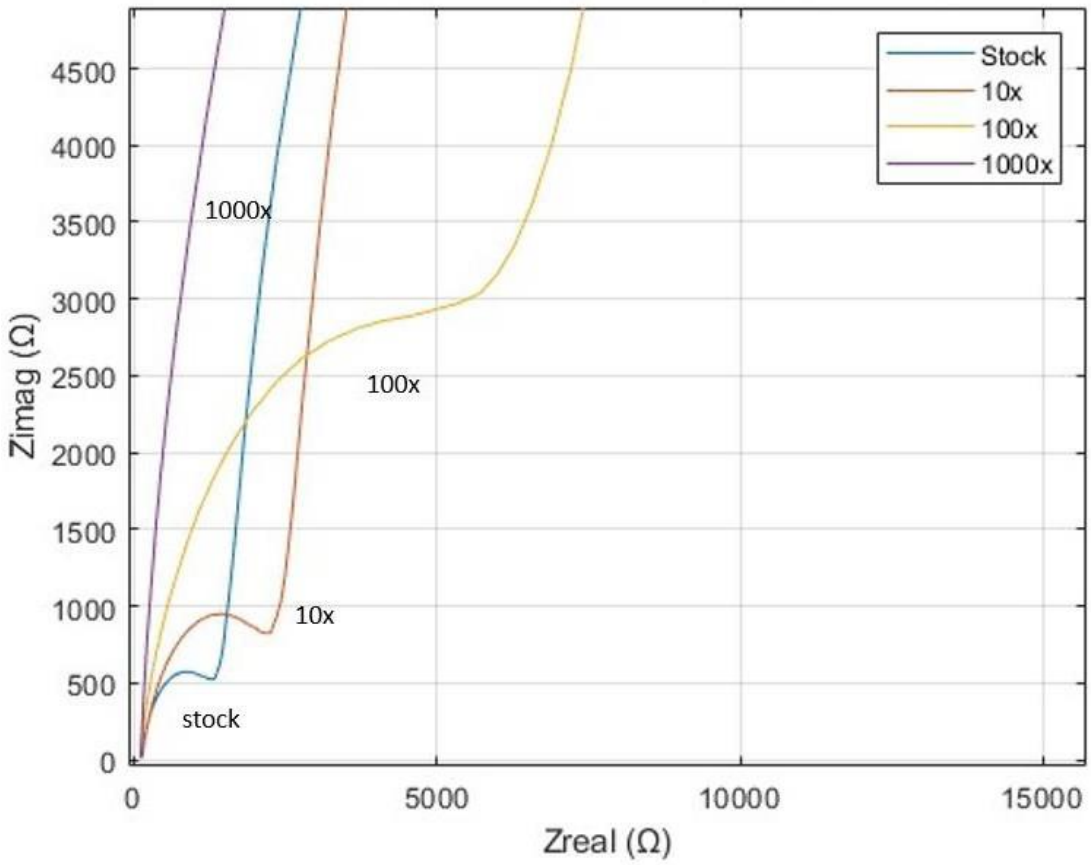

Figure 9 EIS Graph of the Electrochemical Response of SARS-CoV-2 Detection at Stock, 10x, 100x and 1000x Dilutions

The proposed sensor was used to detect SARS-CoV-2 in concentration range from1000x to the stock. As can be seen in Figure 8, the higher the concentration of SARS-CoV-2, the greater the redox response, which implies that an increase in virus concentration leads to a greater extent of redox reactions involving the virus. As can be seen in Figure 8, there is no clear redox peaks associated with SARS-CoV-2 with concentration of 1000x. The EIS analysis was used to further study the interaction between different concentrations of SARS-CoV-2 and the immobilized ACE2 enzyme on the electrode surface. As the virus concentration varied, the Nyquist plots derived from the EIS measurements revealed intriguing tendencies regarding the R_{ct}. The Nyquist plot for the stock COVID concentration displayed the smallest semicircle, corresponding to the lowest R_{ct}. This indicates that the electron transfer process was most effective at this concentration, most likely due to the optimal interaction between the virus and the

immobilized ACE2 enzyme (Ortiz-Aguayo & Valle, 2018). The low R_{ct} value indicates a high rate of charge transfer at the electrode surface, which is commonly associated with effective detection in electrochemical biosensors (Brett, 2022). As the virus concentration was decreased to 10x, 100x, and 1000x, the semicircle in the Nyquist plot (and consequently the R_{ct}) also grew. This suggests that the process of charge transfer became less effective at these lower concentrations. These results reveal that the utilized method for SARS-CoV-2 detection is responsive to concentration changes.

5.5 Calibration curve

Both reduction and oxidation reactions (i.e., redox reactions) exhibited in the cyclic voltammogram were used to quantify the redox response of the sensor (ΔA), which arises from the redox reactions of functional groups on SARS-CoV-2. The redox response was obtained from the difference in current at the oxidation and reduction peaks.

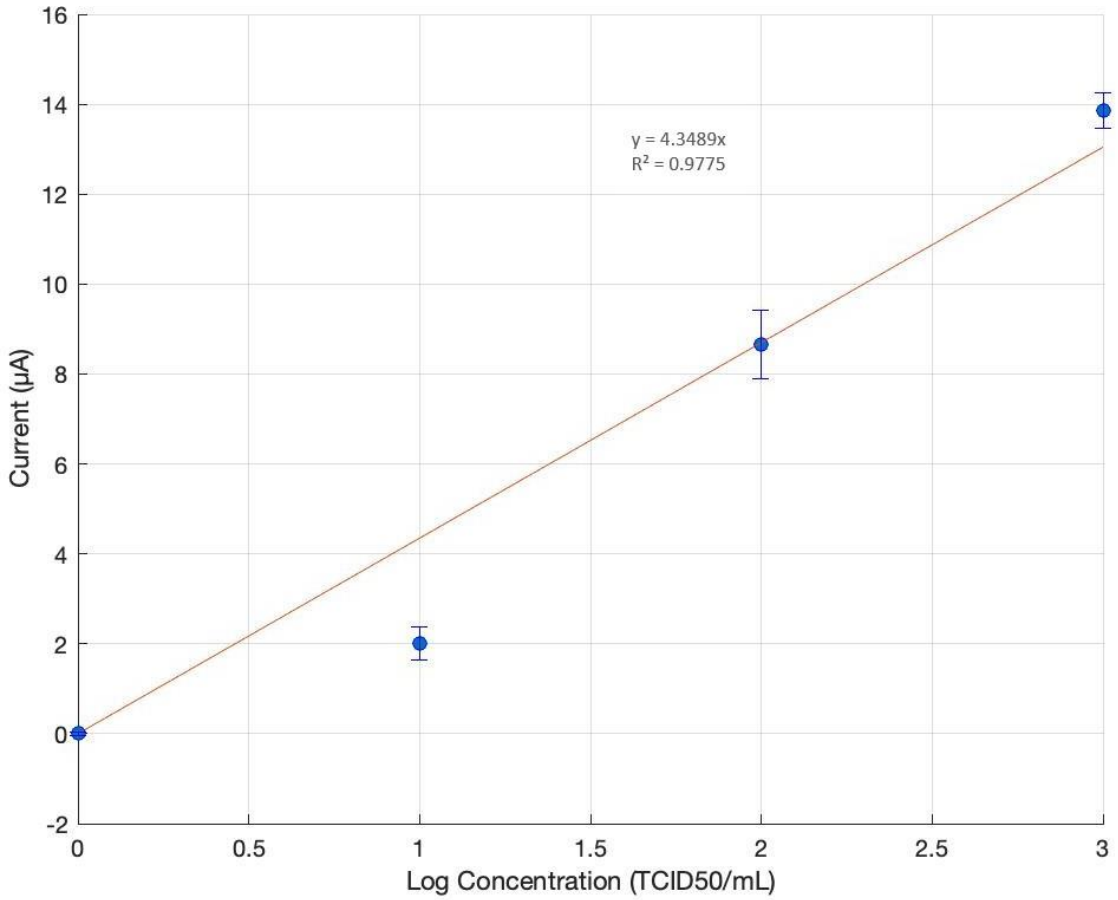

Figure 10 Calibration Curve graph relating the redox current with the virus concentration

The graph illustrates the relationship between the aforementioned SARS-CoV-2 concentrations and the corresponding redox response. The x-axis represents the logarithmic concentration of SARS-CoV-2, while the y-axis represents the redox response. There is a substantial correlation between the two variables, as indicated by the R^2 value of 0.9637. The liner equation is y=4.35x

5.6 Scan Rate Analysis of Stock SARS-CoV-2

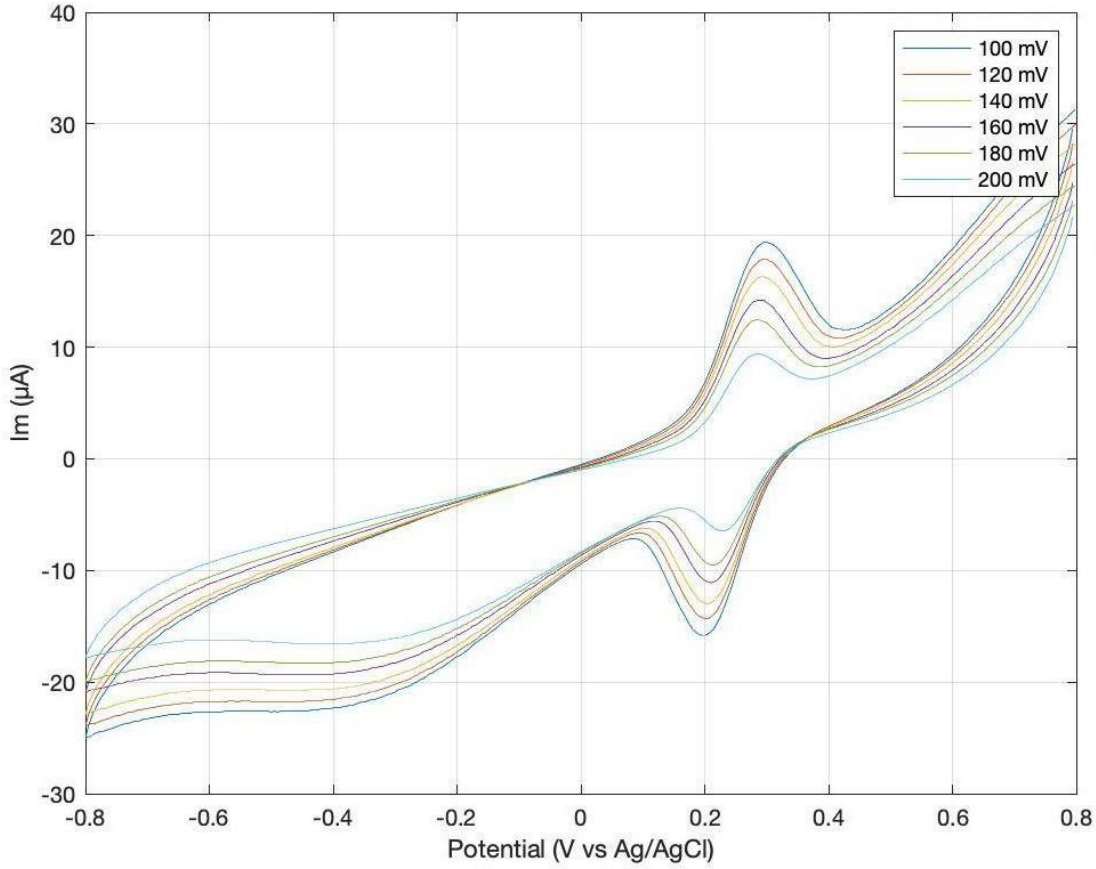

Figure 11 CV Graph depicting the Scan Rates of Stock SARS-CoV-2

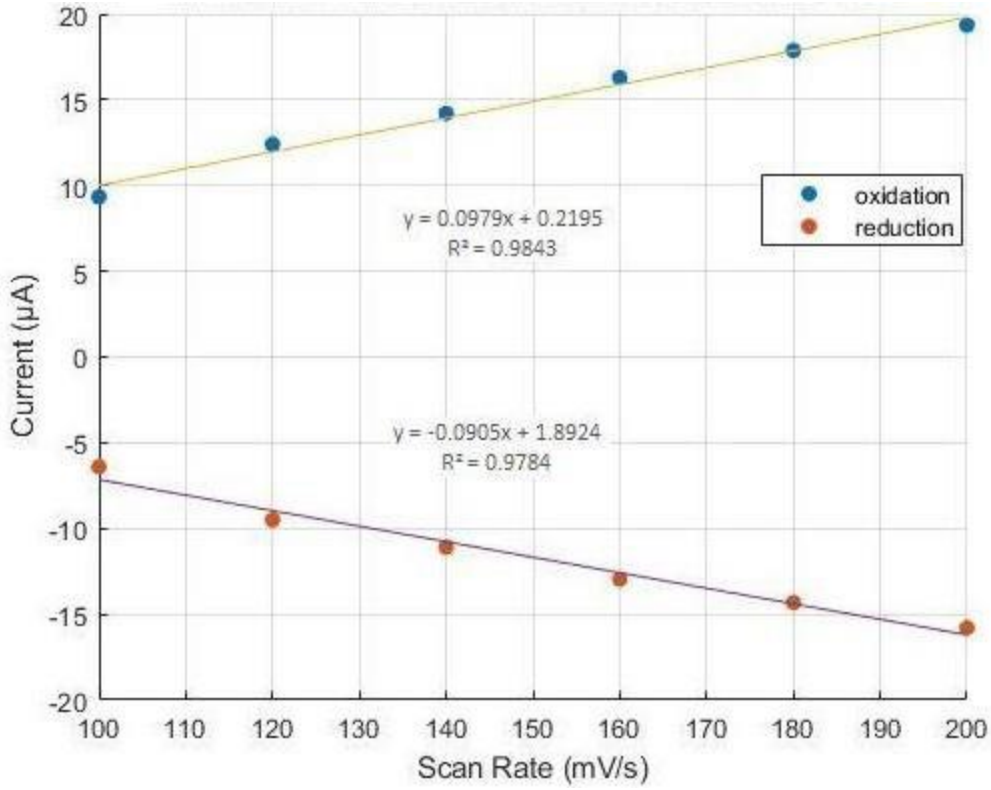

Figure 12 Oxidation and Reduction relationship with increasing scan rate

The kinetics of the electrochemical reaction was examined by altering the scan rate (ν) between 100 mV/s and 200 mV/s during the CV analysis of the sensor. Figure 11 highlights that as the scan rate escalated, both anodic and cathodic peak currents correspondingly increased gradually. Figure 12 emphasizes the linear relationship between the scan rate and the peak current response of the sensor, suggesting the electron transfer is a standard surface-controlled electrochemical process. (Ghaedamini.H et al 2023)

As revealed in Figure 11, with the increase of the scan rate, the cathodic and anodic peak potentials moved steadily towards negative and positive values, respectively, thereby increasing the peak-to-peak separation. Furthermore, the change in anodic peak current (ΔIpa) was not identical to the change in cathodic peak current (ΔIpc). This outcome suggests that the redox reaction is quasi-reversible. In cyclic voltammetry (CV), the scan rate is a crucial parameter that can considerably affect the shape and location of peaks on the CV plot. (Ghaedamini.H et al 2023)

The scan rate represents the rate at which the potential is swept across the range of interest. When the scan rate is increased, the system is given less time to achieve equilibrium at each potential. As observed, this can lead to increased peak currents. This is because the rate of electron transfer (which is proportional to the current) must increase in order to keep up with the increased potential change.

The fact that the peaks became more pronounced with increasing scan rates suggests that the redox reactions in the system are not in equilibrium and are kinetically controlled. This is a common finding in CV experiments and is consistent with electrochemical principles.

5.7 Viral Sensitivity – H1N1/SARS-CoV-2

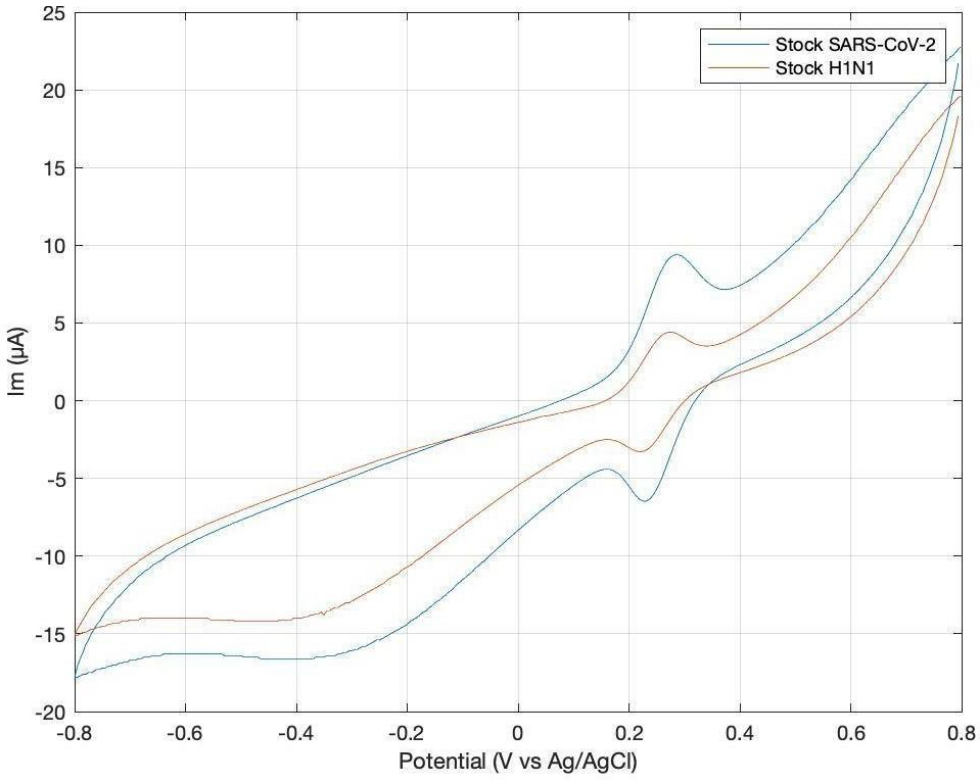

Figure 13 CV graph showing SARS-CoV-2 detection in relation to H1N1

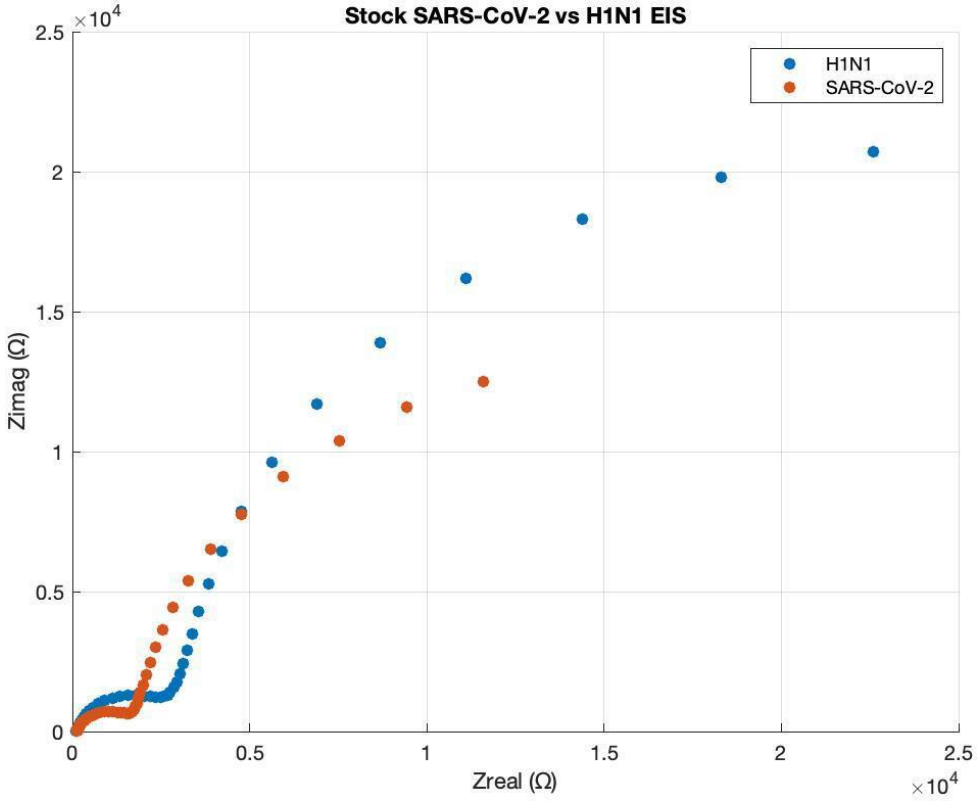

Figure 14 EIS Graph showing SARS-CoV-2 Detection in relation to H1N1

In this comparative experiment to determine the selectivity of our biosensor stock solutions of SARS-CoV-2 and H1N1 tested where SARS-CoV-2 has a concentration of 1.02*10^8 TCID50/mL and H1N1 has a concentration of 3*10^8 TCID50/mL. SARS-CoV-2 had a larger oxidation and reduction peak in the CV measurements and a smaller charge transfer resistance (Rct) in the EIS measurements when compared to H1N1. This indicates that the electron transfer process was more effective for SARS-CoV-2, due to a stronger interaction between SARS-CoV-2 and the immobilized ACE2 enzyme on the sensor surface. This is consistent with what is known about the biology of SARS-CoV-2, which utilizes ACE2 as its primary receptor to enter human cells (Temmam et al., 2022).

Although the sensor also detected H1N1, the signal was weaker than that of SARS-CoV-2. This may be the result of a reduced affinity between H1N1 and the ACE2 enzyme,

which results in a less efficient electron transfer and a larger Rct. Even though ACE2 is not the primary receptor for H1N1, some interaction may still take place, resulting in a detectable signal (Karaman et al., 2021).

These results indicate that the sensor is more sensitive to SARS-CoV-2 than it is to H1N1, possibly owing to the specific spike protein interaction between SARS-CoV-2 and the ACE2 enzyme. This is an encouraging finding because it suggests that the sensor could be used to detect SARS-CoV-2 in a mixture of other viruses (Yang et al., 2021). It is crucial to note, however, that these are preliminary findings, and that additional research is required to confirm these results and fully comprehend the underlying mechanisms. For instance, it would be intriguing to examine how the sensor response varies with various virus concentrations and to compare the sensor performance to that of other detection methods (Drobysh et al., 2022).

Chapter 7

7. Conclusion

This thesis concludes with the development and validation of an innovative electrochemical biosensor for detecting SARS-CoV-2. Using aryl diazonium salt-grafted carbon electrodes, the biosensor has demonstrated promising responsiveness to variations in virus concentration.

Using Electrochemical Impedance Spectroscopy (EIS), the effective immobilization of the aryl diazonium salt, ACE2 enzyme, and SARS-CoV-2 was confirmed, with results consistent with Cyclic Voltammetry (CV) findings. The electron transfer process was determined to be most efficient at the stock concentration of COVID, most likely due to the optimal interaction between the virus and the immobilized ACE2 enzyme. As the virus concentration decreased, however, the effectiveness of charge transfer diminished. The cyclic voltammetry was used to quantify the sensor's redox response, which is caused by the redox reactions of functional groups on SARS-CoV-2. The redox response was calculated using the current difference between the oxidation and reduction peaks. In addition, the peaks became more pronounced as the scan rate increased, indicating that the system's redox reactions are not in equilibrium and are kinetically controlled. SARS-CoV-2 exhibited a larger oxidation and reduction peak in the CV measurements than H1N1. While additional research is required to fully comprehend the implications of these findings and to improve the proposed biosensor technology, the work presented in this thesis provides a firm foundation for future research in this field. It is hoped that the development of such biosensors will substantially enhance our capacity to manage the pandemic and potentially future outbreaks of a comparable nature.

Chapter 8

8. Future Work

Optimization of Biosensor Sensitivity and Specificity While the biosensor demonstrated selectivity between SARS-CoV-2 and H1N1, additional studies with a broader range of viruses are necessary to assure the biosensor's specificity. Additionally, the biosensor's sensitivity could be optimized to detect even lower pathogen concentrations.

Integration with Microfluidic Systems: The integration of the biosensor with microfluidic systems is a potentially fruitful area for future research. Microfluidic devices, which manipulate small volumes of fluid, can provide benefits such as decreased sample and reagent volumes, accelerated reaction times, and high-throughput screening. This could contribute to the development of a compact, portable device for on-site and real-time detection of SARS-CoV-2, thereby enhancing the biosensor's usability and accessibility. In addition, the combination of microfluidics and the biosensor could enable multiplexed detection, enabling the simultaneous testing of multiple samples or the detection of multiple viruses, which could be particularly useful in epidemiological surveillance and prevalent co-infection situations.

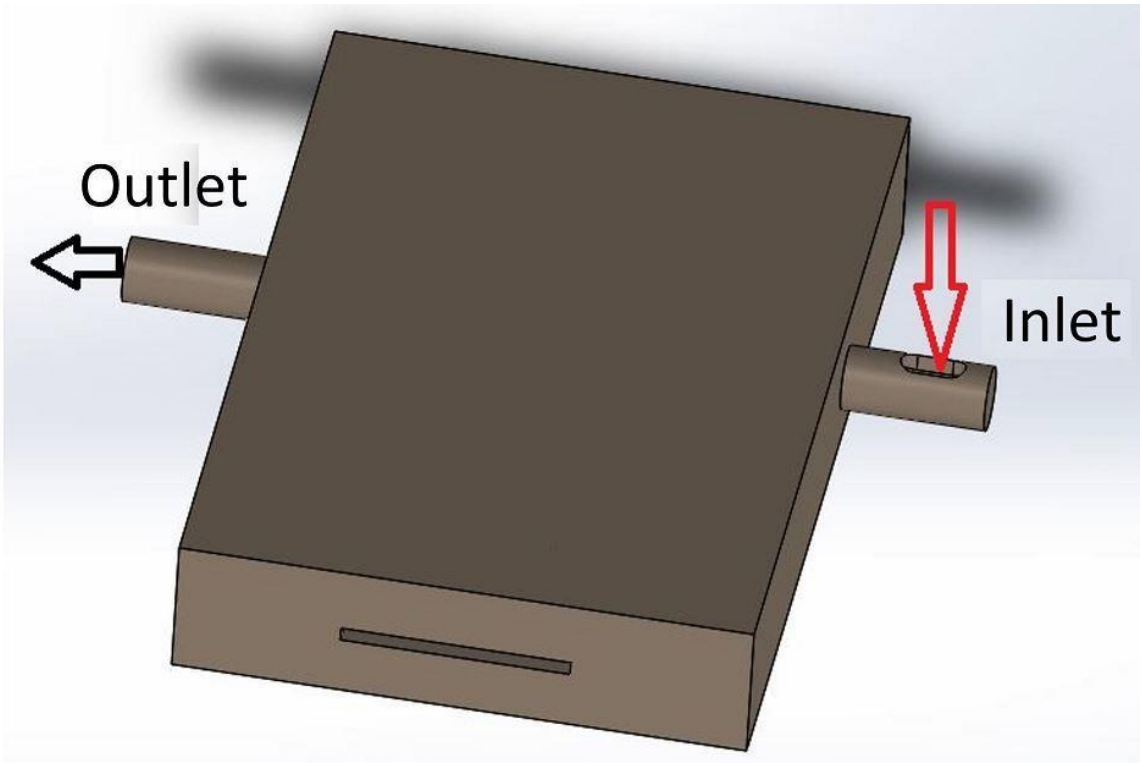

Figure 15 Solidworks design of the proposed Microfluidic device

While testing needs to be done using the microfluidic device, a device was designed through the use of solidworks and we hypothesize that this will allow for a quicker virus incubation time

Real-World Testing: The biosensor was evaluated in a laboratory under controlled conditions. Future research should concentrate on evaluating the biosensor in real-world conditions, utilizing clinical samples.

Scalability and Production: The scalability and cost-effectiveness of biosensor production should be investigated. This would involve investigating methods to mass-produce the biosensor without compromising its efficacy.

Integration with Data Analysis Tools: The biosensor's integration with data analysis tools could allow for real-time monitoring and swift response to changes in virus concentration. This could be beneficial for monitoring the progression of an infection in a patient or the spread of a virus in a community.

References

Jakobsen, K. K., Jensen, J. D., Todsen, T., Lippert, F., Martel, C. J., Klokker, M., & Von Buchwald, C. (2021). Detection of SARS-CoV-2 infection by rapid antigen test in comparison with RT-PCR in a public setting. medRxiv (Cold Spring Harbor Laboratory)

Vadlamani, B. S., Uppal, T., Verma, S. C., & Misra, M. (2020). Functionalized TIO2 Nanotube-Based electrochemical biosensor for rapid detection of SARS-COV-2. Sensors, 20(20), 5871.

Chaimayo, C., Kaewnaphan, B., Tanlieng, N., Athipanyasilp, N., Sirijatuphat, R., Chayakulkeeree, M., Angkasekwinai, N., Sutthent, R., Puangpunngam, N., Tharmviboonsri, T., Pongraweewan, O., Chuthapisith, S., Sirivatanauksorn, Y., Kantakamalakul, W., & Horthongkham, N. (2020). Rapid SARS-CoV-2 antigen detection assay in comparison with real-time RT-PCR assay for laboratory diagnosis of COVID-19 in Thailand.

Hoffmann, M., Kleine-Weber, H., Schroeder, S., Krüger, N., Herrler, T., Erichsen, S., & Müller, M. A. (2020). SARS-CoV-2 cell entry depends on ACE2 and TMPRSS2 and is blocked by a clinically proven protease inhibitor. Cell, 181(2), 271-280.e8.

Ejemel, M., Li, Q., Hou, S., Schiller, Z. A., Tree, J. A., Wallace, A., Amcheslavsky, A., Yilmaz, N. K., Buttigieg, K., Elmore, M. J., Godwin, K., Coombes, N., Toomey, J. R., Schneider, R., Ramchetty, A. S., Close, B. J., Chen, D. Y., Conway, H. L., Saeed, M., . . . Wang, Y. (2020). A cross-reactive human IgA monoclonal antibody blocks SARS-CoV-2 spike-ACE2 interaction. Nature Communications,

Wang, Q., Zhang, Y., Wu, L., Niu, S., Song, C., Zhang, Z., Lu, G., Qiao, C., Hu, Y., Yuen, K., Wang, Q., Zhou, H., Yan, J., & Qi, J. (2020). Structural and functional basis of SARS-COV-2 entry by using human ACE2. Cell, 181(4), 894-904.e9

Tan, C. W., Chia, W. N., Qin, X., Liu, P., Chen, M., Tiu, C., Hu, Z., Chen, V. C. W., Young, B. E., Sia, W. R., Tan, Y. J., Foo, R., Yi, Y., Lye, D. C., Anderson, D. E., & Wang, L. (2020). A SARS-CoV-2 surrogate virus neutralization test based on antibody-mediated blockage of ACE2–spike protein–protein interaction

Shang, J., Ye, G., Shi, K., Wan, Y., Luo, C., Aihara, H., ... & Li, F. (2020). Structural basis of receptor recognition by SARS-CoV-2. Nature, 581(7807), 221-224

Xia, S., Liu, M., Wang, C., Xu, W., Lan, Q., Feng, S., ... & Lu, L. (2020). Inhibition of SARS-CoV-2 (previously 2019-nCoV) infection by a highly potent pan-coronavirus fusion inhibitor targeting its spike protein that harbors a high capacity to mediate membrane fusion. Cell research, 30(4), 343-355.

Tai, W., He, L., Zhang, X., Pu, J., Voronin, D., Jiang, S., ... & Du, L. (2020). Characterization of the receptor-binding domain (RBD) of 2019 novel coronavirus: implication for development of RBD protein as a viral attachment inhibitor and vaccine. Cellular & Molecular Immunology, 17(6), 613-620.

Asselta, R., Paraboschi, E. M., Mantovani, A., & Duga, S. (2020). ACE2 and TMPRSS2 variants and expression as candidates to sex and country differences in COVID-19 severity in Italy. Aging (Albany NY), 12(11), 10087–10098

Zhang, Y., Odiwuor, N., Xiong, J., Sun, L., Nyaruaba, R. O., Wei, H., & Tanner, N. (2020). Rapid Molecular Detection of SARS-CoV-2 (COVID-19) Virus RNA Using Colorimetric LAMP. MedRxiv

Falzone, L., Musso, N., Gattuso, G., Bongiorno, D., Palermo, C. I., Scalia, G., Libra, M., & Stefani, S. (2020). Sensitivity assessment of droplet digital PCR for SARS-CoV-2 detection. International Journal of Molecular Medicine, 46(3), 957–964

Suo, T., Liu, X., Feng, J., Guo, M., Hu, W., Guo, D., Ullah, H., Yang, Y., Zhang, Q., Wang, X., Sajid, M., Huang, Z., Deng, L., Chen, T., Liu, F., Xu, K., Liu, Y., Zhang, Q., Liu, Y., & Zhao, Y. (2020). ddPCR: a more accurate tool for SARS-CoV-2 detection in low viral load specimens. Emerging Microbes & Infections, 9(1), 1259–1268

Barra GB, Santa Rita TH, Mesquita PG, Jácomo RH, Nery LFA. Analytical Sensitivity and Specificity of Two RT-qPCR Protocols for SARS-CoV-2 Detection Performed in an Automated Workflow. Genes (Basel). 2020 Oct 12;11(10):1183.

Lu, R., Wang, J., Li, M., Wang, Y., Dong, J., & Cai, W. (2020). SARS-CoV-2 detection using digital PCR for COVID-19 diagnosis, treatment monitoring and criteria for discharge.

Yu, F., Yan, L., Wang, N., Yang, S., Wang, L., Tang, Y., ... & Wang, F. (2020). Quantitative detection and viral load analysis of SARS-CoV-2 in infected patients.

Tom, M. R., & Mina, M. J. (2020). To interpret the SARS-CoV-2 test, consider the cycle threshold value. Clinical Infectious Diseases, 71(16), 2252-2254.

Corman, V. M., Landt, O., Kaiser, M., Molenkamp, R., Meijer, A., Chu, D. K., ... & Mulders, D. G. (2020). Detection of 2019 novel coronavirus (2019-nCoV) by real-time RT-PCR. Eurosurveillance, 25(3), 2000045.

Kumar, R., Dkhar, D. S., Kumari, R., Mahapatra, S., Kumar, R., & Chandra, P. (2022). Ultrasensitive APTAsensors for the detection of viruses based on Opto-Electrochemical readout systems. Biosensors, 12(2), 81.

Gecgel, O., Ramanujam, A., & Botte, G. G. (2022). Selective electrochemical detection of SARS-COV-2 using deep learning. Viruses, 14(9), 1930.https://www.mdpi.com/2072-666X/12/2/174

Imran, S., Ahmadi, S., & Kerman, K. (2021). Electrochemical biosensors for the detection of SARS-COV-2 and other viruses. Micromachines, 12(2), 174.

Ghani, M. F. A., Nordin, A. N., Zulhairee, M., Nor, A. C. M., Noorden, M. S. A., Atan, M. K. F. M., Rahim, R. A., & Zain, Z. M. (2022). Portable electrochemical biosensors based on microcontrollers for detection of viruses: a review. Biosensors, 12(8), 666.

Ortiz-Aguayo, D., & Valle, M. (2018). Label-Free Aptasensor for Lysozyme Detection Using Electrochemical Impedance Spectroscopy. Sensors, 18(2), 354

Brett, C. (2022). Electrochemical Impedance Spectroscopy in the Characterisation and Application of Modified Electrodes for Electrochemical Sensors and Biosensors. Molecules, 27(5), 1497.

Dhillon, S., & Kant, R. (2017). Theory for electrochemical impedance spectroscopy of heterogeneous electrode with distributed capacitance and charge transfer resistance. Journal of Chemical Sciences, 129(8), 1277-1292

Abe, Y., Hori, N., & Kumagai, S. (2019). Electrochemical Impedance Spectroscopy on the Performance Degradation of LiFePO4/Graphite Lithium-Ion Battery Due to Charge-Discharge Cycling under Different C-Rates. Energies, 12(23), 4507

Mahmoud, K., Hrapovic, S., & Luong, J. (2008). Picomolar detection of protease using peptide/single walled carbon nanotube/gold nanoparticle-modified electrode. ACS Nano, 2(5), 1051-1057.

Heo, N., Zheng, S., Yang, M., Lee, S., Lee, S., Kim, H., Park, J., Lee, C., & Park, T. (2012). Label-Free Electrochemical Diagnosis of Viral Antigens with Genetically Engineered Fusion Protein. Sensors, 12(8), 10097-10108.

Jarocka, U., Sawicka, R., Góra-Sochacka, A., Sirko, A., Zagórski-Ostoja, W., Radecki, J., & Radecka, H. (2014). An Immunosensor Based on Antibody Binding Fragments Attached to Gold Nanoparticles for the Detection of Peptides Derived from Avian Influenza Hemagglutinin H5. Sensors, 14(9), 15714-15728.

Kaushik, A., Yndart, A., Kumar, S., Jayant, R., Vashist, A., Brown, A., Li, C., & Nair, M. (2018). A sensitive electrochemical immunosensor for label-free detection of Zika-virus protein. Scientific Reports, 8(1). Link

Hamidreza Ghaedamini et al 2023 J. Electrochem. Soc. 170 047510

Karaman, C., Yola, B.B., Karaman, O. et al. Sensitive sandwich-type electrochemical SARS-CoV 2 nucleocapsid protein immunosensor. Microchim Acta 188, 425 (2021). https://doi.org/10.1007/s00604-021-05092-6

Rapid, Ultrasensitive, and Quantitative Detection of SARS-CoV-2 Using Antisense Oligonucleotides Directed Electrochemical Biosensor Chip
Maha Alafeef, Ketan Dighe, Parikshit Moitra, and Dipanjan Pan
ACS Nano 2020 14 (12), 17028-17045

Mojsoska, B.; Larsen, S.; Olsen, D.A.; Madsen, J.S.; Brandslund, I.; Alatraktchi, F.A. Rapid SARS-CoV-2 Detection Using Electrochemical Immunosensor. Sensors 2021, 21, 390. https://doi.org/10.3390/s21020390

Temmam, S., Vongphayloth, K., Baquero, E. et al. Bat coronaviruses related to SARS-CoV-2 and infectious for human cells. Nature 604, 330–336 (2022).

Yang, Y., Peng, Y., Lin, C. et al. Human ACE2-Functionalized Gold "Virus-Trap" Nanostructures for Accurate Capture of SARS-CoV-2 and Single-Virus SERS Detection. Nano-Micro Lett. 13, 109 (2021).

Drobysh, M.; Ramanaviciene, A.; Viter, R.; Chen, C.-F.; Samukaite-Bubniene, U.; Ratautaite, V.; Ramanavicius, A. Biosensors for the Determination of SARS-CoV-2 Virus and Diagnosis of COVID-19 Infection. Int. J. Mol. Sci. 2022, 23, 666.